Journal Pre-proof

Rhombohedral stacking-faults in exfoliated highly oriented pyrolytic graphite

Filippo Boi , Cheng-Yang Lee , Shanling Wang , Hansong Wu , Lei Li , Lin Zhang , Jiaxin Song , Yixin Dai , Ayoub Taallah , Omololu Odunmbaku , Anna Corrias , Aleksandra Baron-Wiechec , Shuping Zheng , Salvatore Grasso

PII: S2667-0569(24)00026-9
DOI: https://doi.org/10.1016/j.cartre.2024.100345
Reference: CARTRE 100345

To appear in: *Carbon Trends*

Received date: 13 November 2023
Revised date: 12 March 2024
Accepted date: 14 March 2024

Please cite this article as: Filippo Boi , Cheng-Yang Lee , Shanling Wang , Hansong Wu , Lei Li , Lin Zhang , Jiaxin Song , Yixin Dai , Ayoub Taallah , Omololu Odunmbaku , Anna Corrias , Aleksandra Baron-Wiechec , Shuping Zheng , Salvatore Grasso , Rhombohedral stacking-faults in exfoliated highly oriented pyrolytic graphite, *Carbon Trends* (2024), doi: https://doi.org/10.1016/j.cartre.2024.100345

Rhombohedral stacking-faults in exfoliated highly oriented pyrolytic graphite

Filippo Boi[a]*, Cheng-Yang Lee[a], Shanling Wang[b], Hansong Wu[a], Lei Li[c], Lin Zhang[a], Jiaxin Song[a], Yixin Dai[a], Ayoub Taallah[a], Omololu Odunmbaku[d], Anna Corrias[e], Aleksandra Baron-Wiechec[f], Shuping Zheng[b] and Salvatore Grasso[g*]

[a]College of Physics, Condensed Matter Group, Sichuan University, Chengdu, China.

[b]Analytical & Testing Center, Sichuan University, Chengdu, China.

[c]Institute of Atomic and Molecular Physics, Sichuan University, Chengdu, China.

[d]MOE Key Laboratory of Low-grade Energy Utilization Technologies and Systems, CQU-NUS Renewable Energy Materials & Devices Joint Laboratory, School of Energy and Power Engineering, Chongqing University, Chongqing 400044, China.

[e]School of Chemistry and Forensic Science, University of Kent, Canterbury, UK

[f]Guangdong Technion-Israel Institute of Technology (GTIT), Shantou, China

[g]Queen Mary University of London, School of Engineering and Materials Science, UK

*Corresponding authors email: f.boi@scu.edu.cn, s.grasso@qmul.ac.uk

Abstract

The recent observation of possible granular superconductivity in highly oriented pyrolytic graphite (HOPG) has attracted significant research interest. Here we report a novel investigation on the structural-properties of exfoliated-HOPG. We investigated two types of exfoliation methods, involving either a full (method-1) or partial (method-2) contact between adhesive tape and the main HOPG. Structural characterization was obtained by employing X-ray diffraction (XRD), Raman spectroscopy and electron microscopy (SEM). In particular, Raman point and mapping spectroscopy revealed significant structural-transitions from ABA (Bernal) to ABC (rhombohedral) stacking (stacking-faults), in those samples obtained with the method-2. Interestingly, strained regions exhibiting structural-deformations with a ridge-like morphology were reproducibly identified. The acquired Raman-spectra revealed a local enhancement of the D and D' bands-intensity together with contributions arising from Electronic Raman Scattering (ERS) across the band-gap of rhombohedral-graphite, at middle (~1870 cm^{-1}) and high (~ 2680 cm^{-1}) frequency. HRTEM of the samples produced with the method-2 allowed also for the identification of local-coexistence of ripplocation-like defects with moiré superlattices, an indicator of non-uniform c-axis configuration.

1 Introduction

The recent identification of possible high temperature superconductive effects in highly oriented pyrolytic graphite (HOPG) has attracted significant scientific and technological attention [1-9]. The grain boundaries of HOPG have been often described using a quasi-two-dimensional model established by Burgers–Bragg–Read–Shockley [6]. The investigation of tilted and/or rotated stacking-faults in this class of materials contributed to the identification of unusual local superconductive effects at high temperature [1-9]. Significant electronic contributions arising from edge-dislocations (tilting angle $\theta_{c\text{-}axis} \neq 0$), or screw dislocations (twist-angle $\theta_{twist} \neq 0$) have been proposed [6]. The existence of a network of line defects with flat bands has been predicted at the interfaces between slightly twisted graphene layers ($\theta_{twist} \sim 1°$[6], within HOPG interfaces).

The presence of insulating states, moiré superlattices and logarithmic van Hove singularities has also been demonstrated using scanning tunnelling microscopy/spectroscopy (STM/S) [14, 15]. The properties of multilayer graphene, HOPG and graphite have been reported to be strongly dependent on the local arrangement of the graphene interfaces [4-15]. Annealing HOPG at T ~ 800 K under experimental conditions involving both He exchange-gas and vacuum has been shown to yield unusual ferromagnetic to superconductive-like transitions [1-2]. Furthermore, magnetization signals, which resemble those of granular superconductors, have been reported in samples exhibiting dislocation-rich interfaces, at temperatures as high as ~300-350K [5]. The existence of spontaneous currents, induced at specific Josephson coupled interfaces within the graphite matrix, has also been proposed by Precker et al. [7,8] and Ballestar et al. [9]. In these systems, the control of the relative abundance of the rhombohedral stacking-faults has frequently been indicated as a key parameter triggering the superconductivity [4,7,8,9].

Recently, reproducible identification of rhombohedral stacking-order within comparable systems has also been demonstrated by Yang et al. [10], Henni et al. [11], Shi et al. [12], Wu et al. [13] and Boi et al. [15]. Together with these findings, low-temperature superconductive effects have been identified in other defect-rich graphite samples [16] and in graphene devices exhibiting tuneable twisted interfaces. Significant differences between the two systems (defect-rich graphite and twisted-

graphene) have been detected; in particular the critical superconductive temperature (T_c) of twisted graphene systems has been reported at T ~1-3 K [17-20]. The coexistence of both hexagonal moiré-superlattices and rhombohedral graphitic phases (i.e. as adjacent stacking-faults within the Bernal ABA matrix of HOPG) has been indicated as an additional factor which may contribute in triggering localized superconductive features (i.e. persistent currents) at high temperature [4, 6-9,13].

The presence of possible contributions arising from other category of defects has also been proposed by Arnold et al. [16], revealing low-temperature local superconductivity with T_c~ 14K (through magnetic-field-dependent point-contact spectroscopy) [16].

In this work, we present a major focus on the characteristic role of exfoliation in the controlled deformation of HOPG lamellae, with a discussion on the structural properties of these materials. Structural characterization was obtained by employing X-ray diffraction (XRD at T~ 300K), Raman mapping spectroscopy and electron microscopy (SEM). We investigated two types of exfoliation methods, involving either a full (method-1) or partial (method-2) contact between adhesive tape and the main HOPG. Raman point- and mapping- spectroscopy revealed a significant stabilization of rhombohedral stacking-order in those samples obtained with the method-2, with a clear structural-deformation and nucleation of ridge-like defective morphologies, as revealed by both SEM and Optical microscopy acquisitions. Significant band-contributions arising from electronic Raman scattering (ERS) across the band-gap of rhombohedral-graphite (acquired from those regions exhibiting structural ridge-like deformations) were observed, with a dependence on the intensity of the D and D' components. In addition, further characterization of the sample's produced with method-2, with TEM, HRTEM and SAED evidenced the nucleation of ripplocation-like low-dimensional defects, also in local coexistence with moiré superlattices. SAED characterization revealed a non-uniform arrangement of the c-axis within the analysed regions.

2 Experimental

HOPG samples with variable dimensions of grade A (purity >99.99%) were purchased from XFNANO, INC China. The dimensions of each sample were of 5 x 5 x 1 mm (mosaic angles of 0.5° ± 0.2°, according to manufacturer specifications).

Exfoliated lamellae were prepared by employing two different tape-exfoliation methods, involving a full (*method-1*) or partial (*method-2*) contact of the tape with HOPG, see Fig.2. The thickness of the produced lamellae was in the order of 15-20 μm. The XRD measurements were performed (at room temperature) by employing a PANalytical Empyrean powder X-ray diffractometer (Cu K-α_1, λ =0.15406 nm), equipped with a primary Johansson monochromator, an Oxford Cryosystems PheniX cryostat operating under vacuum below 10^{-2} Pa, and a X'celerator linear detector. Point Raman Spectroscopy acquisitions were carried out in a custom-built Raman system using a triple grating monochromator (Andor Shamrock SR-303i-B, EU) with an attached EMCCD (ANDOR Newton DU970P-UVB, EU), excitation by a solid-state laser at 532 nm (RGB lasersystem, NovaPro 300 mW, Germany) and collection by a 20×0.28 NA objective (Mitutoyo, Japan). Raman mapping measurements were performed by employing a Raman system, HR Evolution, Horiba Jobin Yvon and a LabRAM Soleil, from HORIBA FRANCE SAS (laser wavelength, λ~ 638 nm) with a laser spot diameter of 0.65 microns.

TEM, HRTEM and selective area electron diffraction (SAED) characterization of manually exfoliated thin lamellae (method-2 in Fig.2) were performed by employing a 200 kV American FEI Tecnai G2F20. The sample was inserted into a double folding copper grid, equipped with a formvar support film stabilized with carbon (purchased from the company EMCN, Henan Zhongjingkeyi Import and Export Co., Ltd) for the analyses of the lamella's top section. Fourier transform analyses (performed with the software Digital Micrograph) allowed to identify the unusual super-periodicities observable in some of the analysed interfaces. SEM acquisitions were obtained by employing a JSM-7500F at 5–20 kV.

3 Results and Discussion

XRD analyses of the pristine as purchased HOPG revealed intense 002 and 004 reflections which originate from the multilayered hexagonal structure of the sample, observable in Fig.1A-B, while no contributions from rhombohedral stacking-order were identified at 43 and 46 2θ degrees (Fig.1C). Typical Raman spectroscopy point-acquisitions are shown in Fig.1D.

The lamellae were then prepared by employing the two methods of tape-exfoliation, involving a full or partial tape-contact with the HOPG surface, as shown in the

schematic of Fig.2. Insights on the morphological and structural properties of the lamellae were obtained by employing Raman point and mapping spectroscopy and electron microscopy (SEM). In particular, the contrast between the lamellae morphologies obtained with the method-1 and -2 are shown in Fig.3-4 and Fig.5-8 respectively.

Raman point/map acquisitions from the samples produced with the method-1 revealed a dominant Bernal graphitic arrangement (within the layers of the lamellae), with a dominant smooth-morphology. This is observable in the Raman point- and mapping-spectroscopy analyses presented in Fig.3A,B and Fig.3C-E respectively, and in the SEM micrograph presented in Fig.3F. Interestingly, we notice also the appearance of defective-regions (see optical micrograph in inset of Fig.4A), which are observable within local regions of the sample, as demonstrated also in Fig.S3. The Raman point and map-acquisitions presented in Fig.4A,B and Fig.4C-E (scale bars correspond to 2 μm) provide a typical example of the structural characterization of these defects. The Raman maps in Fig.4C-E present the spatial variation of the areas of the D, G+D' and 2D bands. Interestingly, it is possible to identify an enhancement of the contribution from the left-shoulder of the 2D band, in proximity of the defect-boundaries, as shown also in the Raman map (inset) of Fig.4B where the spatial variation of the ratio of the two component's areas (of the 2D band) is presented. The morphological aspect of the defective-region is observable also in the SEM-micrograph presented in Fig.4F.

A significantly different effect was then found in the samples produced with the method-2 (see Figs.5-8), with a structural-deformation resulting from the exfoliation process, which is clearly visible in Figs.5A,B with optical micrographs and in Fig.6 with SEM. The Raman spectroscopy maps in Fig.5C,D illustrate the spatial-variation in the height of the G-band. Examples of weak D-band signals detected in these regions are shown in Fig.5E,F by employing point-spectra acquisition. It is of particular importance the identification of local structural transitions from ABA to ABC stacking, observable in those sample-regions exhibiting ridge-like defect-morphologies which possibly result from the shear-deformation imposed by the exfoliation in the method-2 (see Figs.7,8). Such a structural modification of the lamella has analogy with previous results reported by Freise et al. in presence of compressive shear-deformation [22], indicating an important role of the shear-parameter [22,23]. Previous investigations of structural deformations in molybdenum

disulphide through nanomechanical-cleavage, reported by Tang et al. [24], have also revealed the nucleation of kinks (during bending) as a consequence of competing effects between the bending-strain-energy and the interfacial energy on interlayer-sliding [24]. Interestingly, the analyses of the Raman spectra acquired from those sample regions exhibiting a structural-deformation (Fig.7) show a significant local enhancement in the intensity of the D and D' bands together with the appearance of middle (~1870 cm^{-1}) and high (~ 2680 cm^{-1}) frequency signals, attributable to electronic Raman scattering (ERS) across the band gap of rhombohedral ABC graphite. The intensity of the ERS band was found to be strongly dependent on the amplitude of the D and D' signals from those multilayered regions exhibiting ridge-like defect-morphologies (see Fig.7A-C). This interpretation was also verified by examining those signal contributions arising from the left-shoulder of the 2D band, as shown in Figs.7E,F and Fig.8. The observed contributions arising from the rhombohedral stacking-faults were reproducibly observed in tens of acquisitions, in the frequency range from 1000 to 2000 cm^{-1} and 2000 to 3000 cm^{-1}. The Raman maps in Fig.8B,C evidence the spatial variation of the ratio of the areas of the rhombohedral and Bernal components and highlight the coexistence of the two phases in the produced lamella.

Additional morphological and cross-sectional analyses of this type of lamella's layered structure are shown in Figs.9-11, which show the results of the TEM/HRTEM characterization. In Fig.9C we point out the observation of anomalous doubled SAED patterns appearing within specific regions of the exfoliated sample. Fig.9D,E evidence also the presence of fringes with possible super-periodicities. Interestingly, previous observations of non-hexagonal superlattices have been ascribed to a non-uniform arrangement of the c-axis within the layered structure of the lamella, in presence of local misorientation and stacking disorder between the graphitic-layers [21].

In the attempt to accurately identify the period of the observed fringes, extended interpretation was sought by employing both HRTEM/profile analyses and Fourier transform methodologies. As shown in ESI Fig.S1,2 multiple super-periodicities with period d~ 0.815 nm, d~1.004 nm, d~1.246 nm, d~1.571 nm, d~2.409 nm, d~ 4.171 nm, were identified. An unusual coexistence of wrinkle- and ripplocation-like defect-structures with moiré superlattices was also observed in those thin regions of the lamella observable through HRTEM, as shown in Fig.10,11. SAED analyses of these sample-regions confirmed further the presence of the anomalous doubled diffraction

patterns, as shown in Fig.10G-I and ESI Fig.S2, which we interpret as an indicator of non-uniform c-axis distribution in the analysed sample's areas.

Conclusion

In conclusion, we presented a novel investigation on the structural-properties of exfoliated-HOPG. We investigated two types of exfoliation methods, involving either a full (method-1) or partial (method-2) contact between tape and the main HOPG sample. Structural characterization, obtained by employing XRD, Raman spectroscopy and SEM revealed significant differences between the two methodologies. In particular, Raman point and mapping spectroscopy revealed structural-transitions from ABA (Bernal) to ABC (rhombohedral) stacking (stacking-faults), in the samples obtained with the method-2, with the formation of strained-regions exhibiting structural-deformations, with a ridge-like defective morphology.
HRTEM analyses of sample's produced with the method-2 revealed also the nucleation of low-dimensional defects with a ripplocation- and wrinkle-like morphology. Additional work is however needed to obtain a statistical information on the structural properties of the observed ripplocation-like defects. This aspect will be investigated in the future work.

Conflicts of interest

There are no conflicts of interest to declare

Acknowledgments:

Prof. Filippo Boi is grateful to the financial support from the National Natural Science foundation (NSFC) of China Grant N° 11950410752 and Sichuan University Research Leader fund. We would like to thank Dr. Shanling Wang, Dr. Shuping Zheng, Dr. Wu Li and Dr. Su Yingying of the Analytical and Testing Center of Sichuan University for the TEM, SEM and Raman Spectroscopy work respectively. We also acknowledge Mr. Xiangshang Xiao for his help.

References

[1] Kopelevich Y., Esquinazi P., Torres J. H. S., Moehlecke S. Ferromagnetic- and Superconducting-Like Behavior of Graphite. Journal of Low Temperature Physics 119 (2000) 691-702.

[2] Kopelevich Y., Lemanov V. V., Moehlecke S. and Torres J. H. S. Landau level quantization and possible superconducting instabilities in highly oriented pyrolytic graphite. Physics of the Solid State 41 (1999) 1959-1962.
[3] Brandt N.B., Kotosonov A.S., Kuvshinnikov S.V., Semenov M.V. The possibility of increasing diamagnetic susceptibility of pyrocarbon. JETP letter 29 (1979) 720-722.
[4] Ariskina, R., Stiller M., Precker C.E., Böhlmann W., Esquinazi P.D. On the Localization of Persistent Currents Due to Trapped Magnetic Flux at the Stacking Faults of Graphite at Room Temperature. Materials 2022; 15: 3422.
[5] Scheike T., Esquinazi P., Setzer A., and Böhlmann W. Granular superconductivity at room temperature in bulk highly oriented pyrolytic graphite samples. Carbon 2013; 59:140-149.
[6] Esquinazi P., Heikkilä T. T., Lysogorskiy Y. V., Tayurskii D. A., and Volovik G. E. On the Superconductivity of Graphite Interfaces. JETP Letters 2014; 100: 336–339.
[7] Precker C. E., Esquinazi P. D., Champi A., Barzola-Quiquia J., Zoraghi M., Muiños-Landin S., Setzer A., Böhlmann W., Spemann D., Meijer J., Muenster T., Baehre O., Kloess G. and Beth H. Identification of a possible superconducting transition above room temperature in natural graphite crystals. New J. Phys. 2016;18: 113041.
[8] Precker C. E., Barzola-Quiquia J., Chan M. K., Jaime M., Esquinazi P. D. High-field and high-temperature magnetoresistance reveals the superconducting behavior of the stacking faults in multilayer graphene. Carbon 2023; 203: 462-468.
[9] Ballestar A., Barzola-Quiquia J., Scheike T. and Esquinazi P. Josephson-coupled superconducting regions embedded at the interfaces of highly oriented pyrolytic graphite. New Journal of Physics 2013;15: 023024.
[10] Yang Y., Zou Y.-C., Woods C. R., Shi Y., Yin J., Xu S., Ozdemir S., Taniguchi T., Watanabe K., Geim A. K., Novoselov A. K., Haigh S. J. and Mishchenko A. Stacking Order in Graphite Films Controlled by van der Waals Technology. Nano Lett. 2019; 19: 8526−8532.
[11] Henni Y., Collado H. P. O., Nogajewski K., Molas M. R., Usaj G., Balseiro C. A., Orlita M., Potemski M. and Faugeras C. Rhombohedral Multilayer Graphene: A Magneto-Raman Scattering Study, Nano Lett. 2016; 16: 3710−3716.
[12] Shi Y., Xu S., Yang Y., Slizovskiy S., Morozov S. V., Son S.-K., Ozdemir S., Mullan C., Barrier J., Yin J., Berdyugin A. I., Piot B. A., Taniguchi T., Watanabe K., Fal'ko V. I., Novoselov K. S., Geim A. K. and Mishchenko A. Electronic phase separation in multilayer rhombohedral graphite. Nature 2020; 584: 210–214.
[13] H. Wu, J. Song, S. Wang, J. Wen, A. Gu, Y. Dai, W. Li, H. Zhang and F. S. Boi. Coexistence of crystalline rhombohedral stacking and hexagonal moiré superlattices in exfoliated highly oriented pyrolytic graphite. Materials Today Comm. 2022; 32: 104152.
[14] Brihuega I., Mallet P., González-Herrero H., de Laissardière G. T., Ugeda M. M., Magaud L., Gómez-Rodríguez J. M., Ynduráin F., and Veuillen J.-Y. Unraveling the Intrinsic and Robust Nature of van Hove Singularities in Twisted Bilayer Graphene by Scanning Tunneling Microscopy and Theoretical Analysis. Phys. Rev. Lett. 2012; 109: 196802.

[15] Boi F.S., Song J., Li W., Guo J., Gao S., Wang S., Wen J., Zhang H. Van Hove singularities, moiré-superlattices and rhombohedral stacking in exfoliated sublattices of highly oriented pyrolytic graphite. Materials Today Chemistry 2021; 22:100585.
[16] Arnold F., Nyéki J., Saunders J. Superconducting sweet-spot in microcrystalline graphite revealed by point-contact spectroscopy, JETP Lett. 107 (2018) 577–578.
[17] Cao Y., Fatemi V., Fang S., Watanabe K., Taniguchi T., Kaxiras E. and Jarillo-Herrero P. Unconventional superconductivity in magic-angle graphene superlattices. Nature 2018; 556: 43–50.
[18] Cao Y., Fatemi V., Demir A., Fang S., Tomarken S. L., Luo J. Y., Sanchez-Yamagishi J. D., Watanabe K., Taniguchi T., Kaxiras E., Ashoori R. C. and Jarillo-Herrero P. Correlated insulator behaviour at half-filling in magic-angle graphene superlattices. Nature 2018; 556: 80–84.
[19] Park J. M., Cao Y., Watanabe K., Taniguchi T. and Jarillo-Herrero P. Tunable strongly coupled superconductivity in magic-angle twisted trilayer graphene. Nature 2021; 590: 249–255.
[20] Park, J.M., Cao, Y., Xia, LQ. et al. Robust superconductivity in magic-angle multilayer graphene family. Nat. Mater. 2022; 21: 877–883.
[21] Boi F. S., Shuai G., Wen J. and Wang S. Unusual Moiré superlattices in exfoliated μm-thin HOPG lamellae: An angular-diffraction study. Diamond and Related Materials 2020;108: 107920.
[22] Freise E. J. and Kelly A. The deformation of graphite crystals and the production of the rhombohedral form, The Philosophical Magazine: A Journal of Theoretical Experimental and Applied Physics 1963; 93: 1519-1533.
[23] Nery J. P., Calandra M. and Mauri F. Long-Range Rhombohedral-Stacked Graphene through Shear. Nano Lett. 2020, 20, 7, 5017–5023.
[24] Tang, DM., Kvashnin, D., Najmaei, S. et al. Nanomechanical cleavage of molybdenum disulphide atomic layers. Nat Commun 2014; 5: 3631.

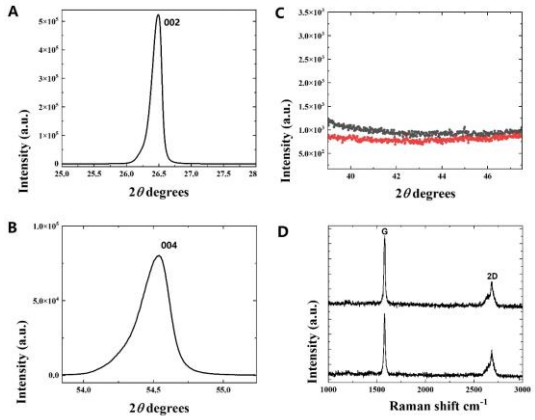

Figure 1: XRD signals acquired from as-purchased HOPG exhibiting typical 002 and 004 reflections (A,B). No contributions from rhombohedral graphite were identified in the pristine sample as shown in C. This interpretation was confirmed by point-Raman spectroscopy measurements, typical examples are shown in D.

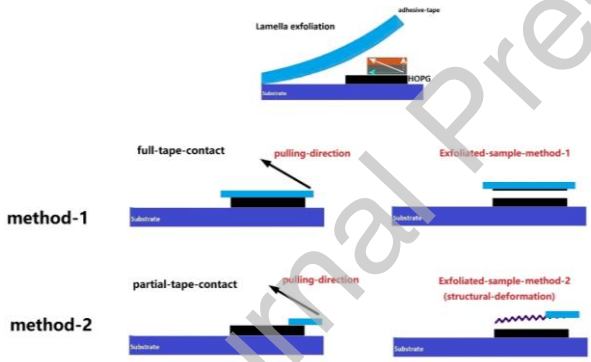

Figure 2: Schematic of the methods used for the lamella exfoliation, from the main HOPG sample. Note in the method-1, a full contact is present between the tape and the HOPG surface. Instead in the method-2, the process of exfoliation involves a partial tape contact and is assisted through the use of flat-tipped tweezers

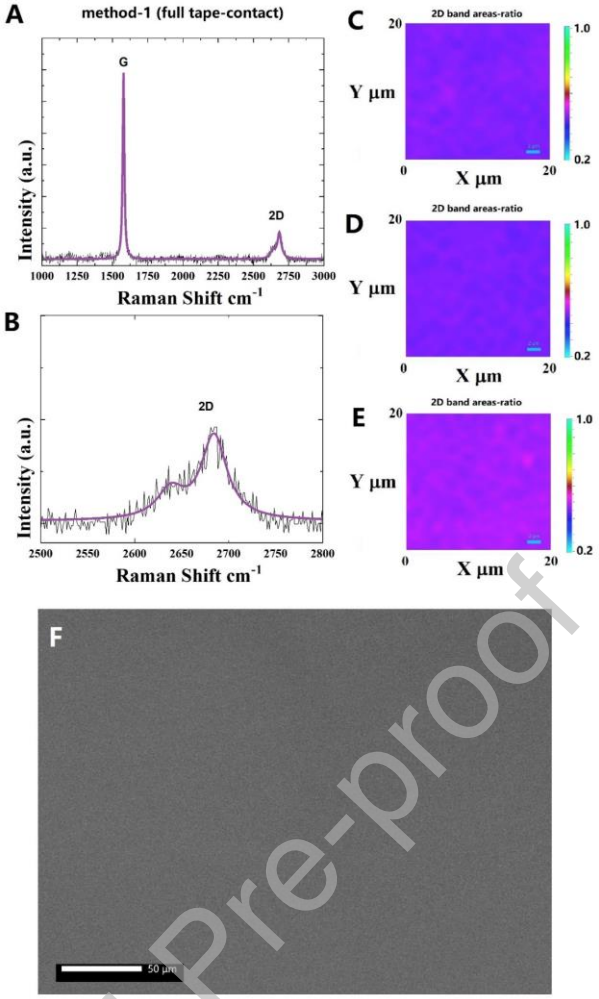

Figure 3: Raman point- (A,B), mapping-spectroscopy (C-E) and SEM (F) characterization of a smooth lamella produced with the method-1, with full tape-contact.

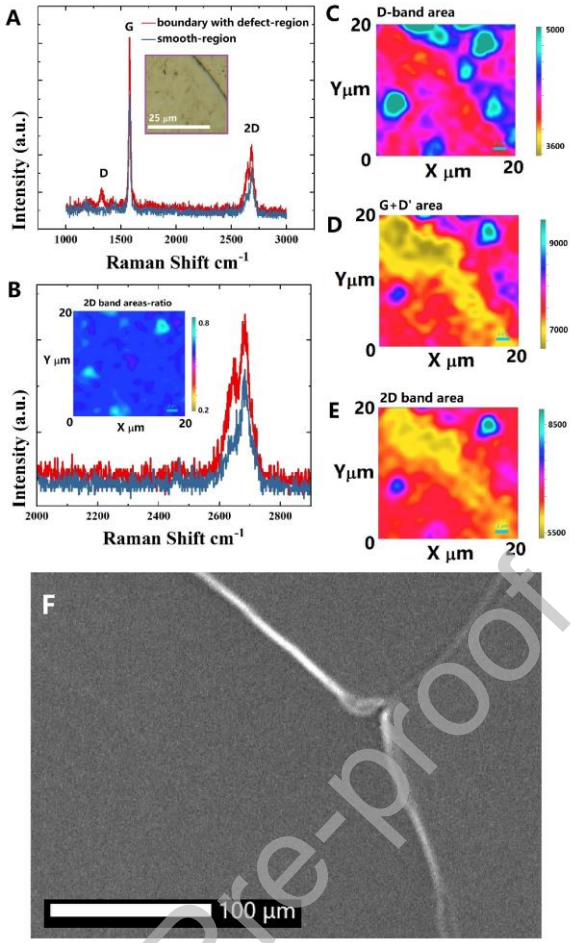

Figure 4: Additional Raman spectroscopy point and map acquisitions performed in proximity of the defective region (see inset in A) created by the method-1 of exfoliation (point spectra in A,B and maps in C-E, B-inset). Examples of this type of defects are shown in the inset in A by optical microscopy and in F, by SEM. The maps presented in C-E (scale bars correspond to 2μm) show the spatial variation of the areas of the D, G+D' and 2D bands. It is noticeable a weak enhancement of the contribution from the left-shoulder of the 2D band in proximity of the defect-boundary region. This local transition is visible in the inset in B, where the spatial variation of the ratio of the two component's areas (of the 2D band) is shown.

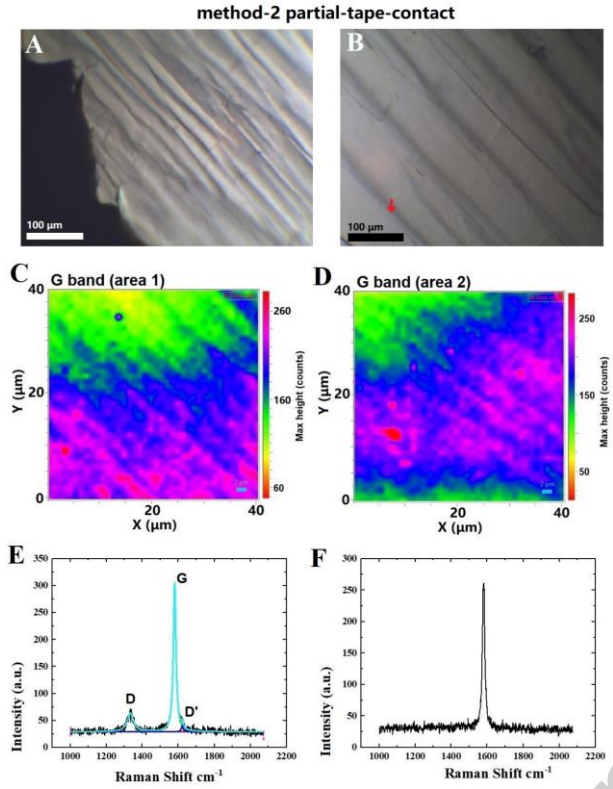

Figure 5: In A, B examples of an irregularly-stacked lamella resulting from manual exfoliation (by employing method-2, with the aid of flat-tipped tweezers). Note the appearance of unusual ridge-like deformation-defects which result from the exfoliation process. In C, D typical Raman spectroscopy spatial maps, evidencing the presence of a spatial-variation in the G-band peak-height. In E, F examples of the point-spectra acquisition See B for typical example of the ridge-like deformation resulting from the method-2 of exfoliation (red arrow).

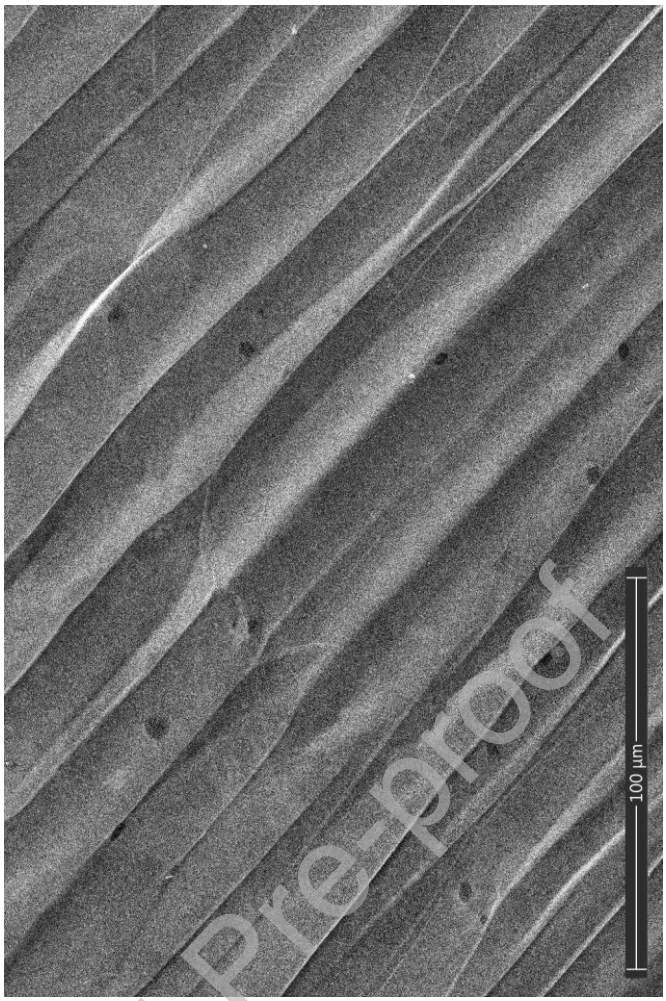

Figure 6: Scanning electron micrograph (SEM) of a typical lamella produced with the method-2, evidencing the formation of ridge-like structures as a consequence of the exfoliation process. The black patches identify regions of local oxidation.

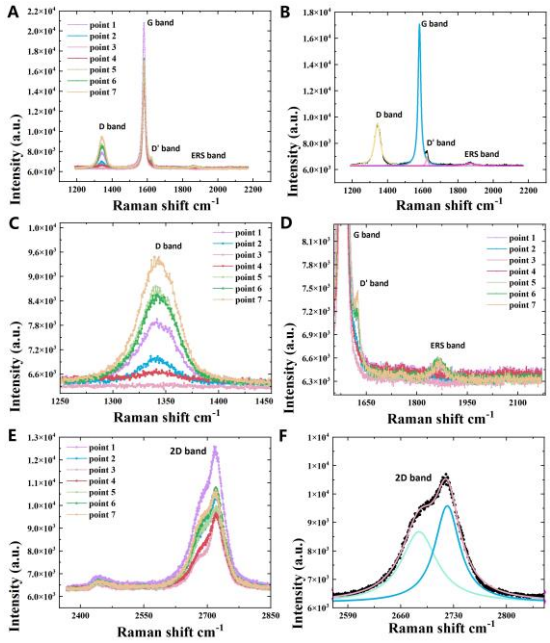

Figure 7: Raman spectra-acquisitions (A-D) revealing a significant local enhancement of the D and D' bands together with the appearance of electronic Raman scattering across the band gap of rhombohedral graphite (D) in those sample regions exhibiting structural-deformation (ridge-like morphologies). In (E,F) note the enhancement of signal contributions arising from the left-shoulder of the 2D band.

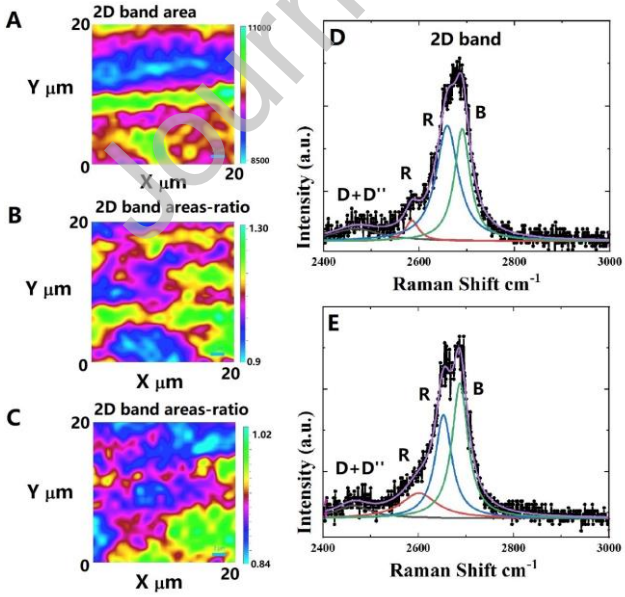

Figure 8: Additional Raman mapping acquisitions in A-C, evidencing the local stabilization of rhombohedral phases in the ridge-like defect-structures observed in

the lamella produced with the method-2. The maps in B,C evidence the spatial variation of the ratio of the areas of the two components of the 2D band identified in D,E resulting from contributions of rhombohedral and Bernal phases (typical examples in D,E). Note the presence of multiple peak-components on the left shoulder of the 2D band-signal, indicative of rhombohedral stacking order in coexistence with the standard Bernal one.

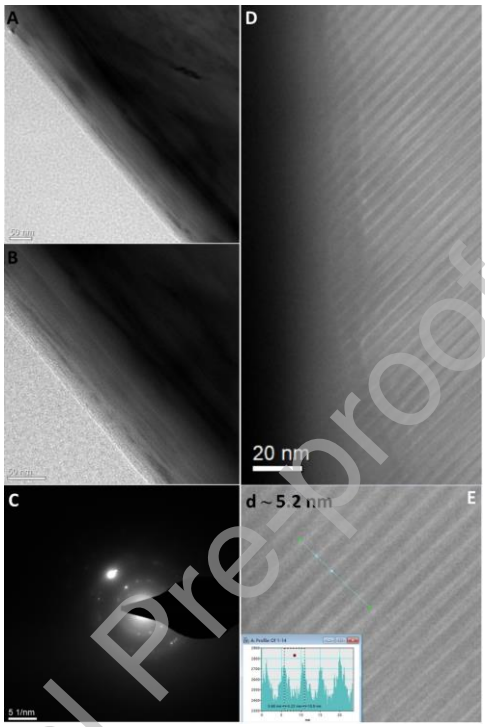

Figure 9: TEM analyses in A,B revealing a variable cross-sectional thickness in the manually exfoliated thin lamella (i.e. method-2, thickness of hundreds of nm). In C, selective area electron diffraction (SAED) analyses revealing the appearance of doubled diffraction patterns which resembles those reported in ref. [21] and possibly indicative of a disordered arrangement of the c-axis. In D, E unusual formation of super-periodicities. A super-periodicity d varying from 4.1 to 5.2 nm could be detected in E.

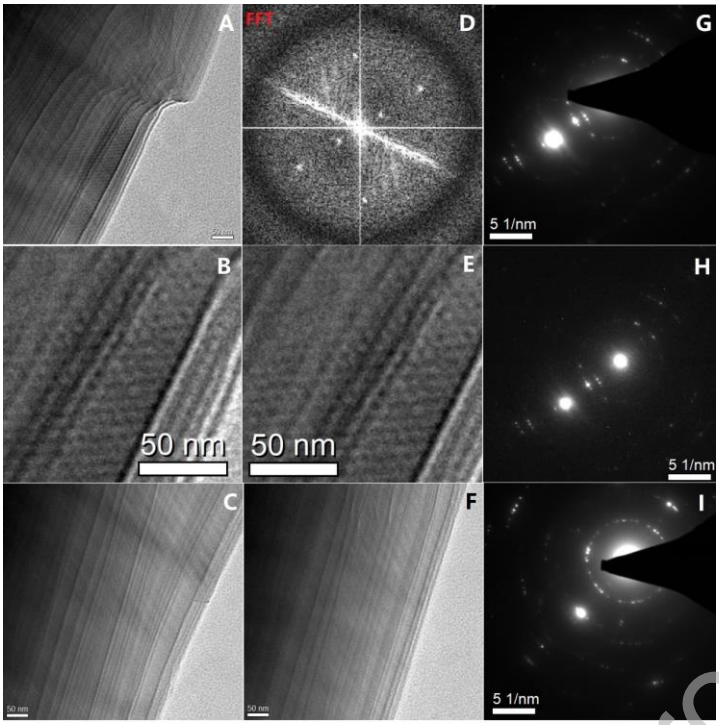

Figure 10: HRTEM analyses revealing the presence of multiple ripplocations and wrinkle-like structures in the lamellae produced with the method-2 of exfoliation. Typical examples are shown in A-C and E,F. The FFT analyses in D evidence the presence of hexagonal super-periodicities (see B and E) compatible with moiré superlattices in coexistence with the ripplocation-like and wrinkle-defects produced by the exfoliation process; with the superlattices periods being D ~ 7.44 nm and D ~21 nm respectively. By employing the equation, $a/2D=\sin(\theta/2)$, with a being the basal lattice constant of HOPG, the following local twisting angles could be identified, namely θ_{twist} ~1.9° and θ_{twist} ~0.67° respectively. The SAED analyses in G-I evidence the presence of anomalous doubled diffraction signals in this category of lamellae, indicative of a disordered arrangement of the c-axis.

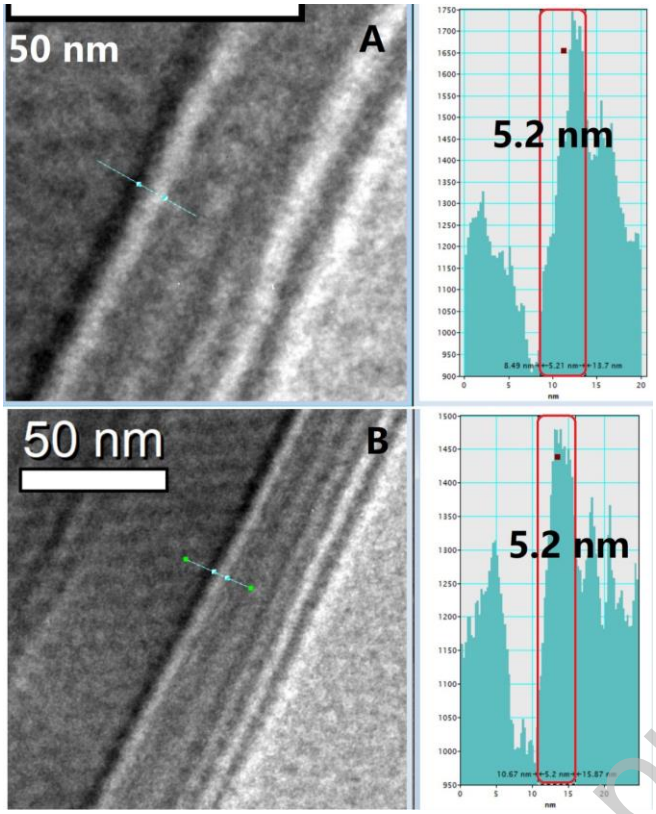

Figure 11: HRTEM analyses of the lamella obtained with the method 2, evidencing the presence of additional wrinkle-like morphologies with a diameter in the order of ~ 5 nm resulting from the exfoliation process.

Declaration of interests:

☒ The authors declare that they have no known competing financial interests or personal relationships that could have appeared to influence the work reported in this paper.

☐The authors declare the following financial interests/personal relationships which may be considered as potential competing interests: